

## The Influence of Agitation Speed on the Morphology and Size Particle

### Synthesis of $Zr(HPO_4)_2 \cdot H_2O$ from Mexican Sand

*García Rosales Genoveva, Ordóñez Regil Enrique,  
Romero Guzmán Elizabeth Teresita\* and Ordóñez Regil Eduardo*

Departamento de Química,  
Instituto Nacional de Investigaciones Nucleares, MEXICO  
Carretera México-Toluca km. 36.5, Apartado Postal 18-1027,  
11801 México D. F., México. Telephone: 525553297200 ext 2266; fax 525553297301.  
E-mail: [etrg@nuclear.inin.mx](mailto:etrg@nuclear.inin.mx); [edo@nuclear.inin.mx](mailto:edo@nuclear.inin.mx)

\* to whom all correspondence should be addressed.

#### **ABSTRACT**

*Mexican zirconium sand has been envisaged like a source of zirconium compounds. The main product obtained is zircon ( $ZrSiO_4$ ), which has a high raw material value. During a mineralogical purification sand process with hydrofluoric acid, a liquor was obtained as the by product. This liquor was dripped over hot phosphoric acid to obtain zirconium hydrogen phosphate  $Zr(HPO_4)_2 \cdot H_2O$  ( $\alpha$ -ZP) which has taken considerably attention due to its wide application. Both products zircon and  $\alpha$ -ZP were analyzed as for structure and purity using analytic techniques. X-Ray diffraction revealed that zircon and  $\alpha$ -ZP were polycrystalline materials. Scanning Electron Microscopy indicated that  $\alpha$ -ZP formed particles and aggregates in different shapes and size distributions depending on the condensing way and the agitation speed. Furthermore, thermogravimetric analysis demonstrated that the  $\alpha$ -ZP phases present different hydrated levels. FTIR spectra were obtained to identify the corresponding P-O stretching vibration from the  $\alpha$ -ZP and the specific surface areas were calculated by BET method.*

**Keywords:** *Zirconium sand; Zirconium phosphates;  $\alpha$ -ZP surface morphology;  $\alpha$ -ZP synthesis.*

#### **1. INTRODUCTION**

The disposition of radioactive wastes is, undoubtedly, one of the more serious environmental problems recognized nowadays. In order to solve it, scientists have studied for several years, the way in which such materials can be stored in a safe form in order to avoid the

radionuclides migration towards the environment. That is the reason why new geological storage sites are under evaluation. Considering the long life time of some alpha emitters, it is interesting to study the possibility of building suitable long term geologic repositories for spent nuclear fuel and high level radioactive wastes. These sites should be reinforced with some adsorbent materials as artificial barriers [1].

Radioactive materials are, in general, natural or synthetic minerals with important surface characteristics, such as stability and chemical reactivity [2]. Early studies were made on the natural apatite whose results suggested some problems due to the dissolution of the materials with pH changes [3]. Due to their abundance in the geosphere, much attention has been paid to the aluminosilicates and clays with a view to finding suitable engineered barriers for radioactive wastes confinement [4, 5]. Recently, phosphated derivatives containing lanthanum, thorium and uranium have been also studied in order to produce stable materials with sorbent properties [6].

It has been observed that zircon exhibits surface properties that could be considerably useful for radioactive wastes storage in a Deep Geological Repository (DGR) [7]. When zirconium rich sand from South Baja California, Mexico, is purified, high quality zircon is obtained as main product with zirconium tetrafluoride as by-product, which added directly to hot phosphoric acid enables to obtain  $\alpha$ -ZP. The  $\alpha$ -ZP is chemically inert at neutral or acid pH, and thermally stable at elevated temperatures [8]. Furthermore, it could be a material of choice as a filler for large scale applications in DGR's due to its stability in a hydrogen-oxygen atmosphere, its low cost and low toxicity [9].

This compound was firstly reported by Clearfield and Stynes in 1964 [10]. After that, several procedures of synthesis had been established [11] by hydrothermal and wet methods, which take many steps to obtain the desired crystallographic phases. This procedure can be considered as an improvement over the soft chemistry method to prepare  $\alpha$ -ZP [2].

The aim of the present work has been not only zircon purification itself but also the synthesis of zirconium hydrogen phosphate  $Zr(HPO_4)_2 \cdot H_2O$ , known as ( $\alpha$ -ZP), on the basis of a non conventional method as well as evaluating the influence of agitation on the formation of different crystalline forms [10].

## 2. EXPERIMENTAL

The beach sand was purified to obtain an interesting commercial product, but the resulting acid liquor can be used to obtain the zirconium hydrogen phosphate, which is a product with technological potential applications. The raw material and byproducts were analyzed for chemical purity and crystallographic structure, by conventional analytical and spectroscopic techniques.

## 2.1. Preparation of Samples

Beach sand from South Baja California in Mexico was sieved and cleaned up with a powerful magnet bar in order to separate the ferric minerals. A 100 g batch of cleaned sand was placed into a Teflon™ beaker, added distilled water just to cover the solid and then 50 mL of concentrated hydrofluoric acid were incorporated. The vessel was placed afterwards on a hot sand bath allowing the gently evaporation of the silicon tetrafluoride. Meanwhile the acid was added continuously so to maintain the original volume for 24 hours, then the suspension was filtered out. The supernatant liquor containing zirconium tetrafluoride was mixed with hot concentrated orthophosphoric acid at manual, 100 rpm, 250 rpm and 500 rpm stirring speeds and boiled in order to avoid HF excess in the reaction medium. After a while, the zirconium hydrogen phosphate was condensed, then centrifuged and finally washed several times with distilled water almost to neutrality.

## 2.2. Chemical characterization

### 2.2.1. X-ray powder diffraction (XRD)

The raw material and the obtained phases were identified by powder X-ray diffraction patterns obtained with a Siemens D-5000 diffractometer coupled to a copper anode X-ray tube ( $\lambda=1.543 \text{ \AA}$ ). The  $K_{\alpha}$  radiation was selected with a diffracted beam monochromator. The XRD peaks were recorded in the  $2\theta$  range of  $4^{\circ}$  to  $70^{\circ}$ . The compounds were identified comparing with the JCPDS cards in the conventional way.

### 2.2.2. Scanning electron microscopy (SEM)

The samples were then mounted directly onto the holders using carbon strips, and covered by a sputtered  $200 \text{ \AA}$  gold layer. The material was analyzed by SEM using a PHILIPS XL-30 in order to observe the surface morphology and microstructure of zirconium phosphate and their behavior under the electron beam. In all cases, the images were taken with the backscattered electrons detector. Elemental composition was also studied by EDS with an EDAX, DX-4 spectrometer.

### 2.2.3. Thermogravimetric analysis (TGA)

The small amount of sample was directly placed onto platinum crucible and the analysis was carried out under  $N_2$  flow at the heating rate of  $10^{\circ}\text{C min}^{-1}$ , in the temperature range from room temperature to  $700^{\circ}\text{C}$ , using a TGA-TDA 51 TA Instruments.

### 2.2.4. Specific surface areas

Specific surface areas were determined by the  $N_2$  Brunauer-Emmett-Teller (BET) method in a surface area analyzer Micromeritics Gemini 2360. The dry and degassed samples were then analyzed using a multipoint  $N_2$  adsorption-desorption method at room temperature.

### 2.2.5. Fourier transform infrared spectroscopy

Infrared analysis was also performed for the solid using an IR spectrophotometer Nicolette 550, with the KBr disc method. The sample was scanned for  $4000\text{ cm}^{-1}$  to  $400\text{ cm}^{-1}$ .

## 3. RESULTS AND DISCUSSION

### 3.1. Purification of Beach Sand

The zirconium sand was analyzed by XRD with the aim of identifying all the mineral species present, showing that zirconia ( $\text{ZrO}_2$ ), JCPDS card 37-1484 [12], silica ( $\text{SiO}_2$ ) JCPDS card 33-1161 and zircon ( $\text{ZrSiO}_4$ ) JCPDS card 06-0266 were the major species while aluminosilicates and ferric oxides appeared only as minor species (Figure 1). The EDS analysis taken from samples confirmed the presence of Al, Fe, Zr, Si and O. The sample morphology showed that, in raw sand, a variety of grain size and shape was present (Figure 2). The hydrofluoric acid method proved, in turn, that its reaction with  $\text{ZrO}_2$  and  $\text{SiO}_2$  excluded zirconium silicate, thus facilitating the purification of the latter.

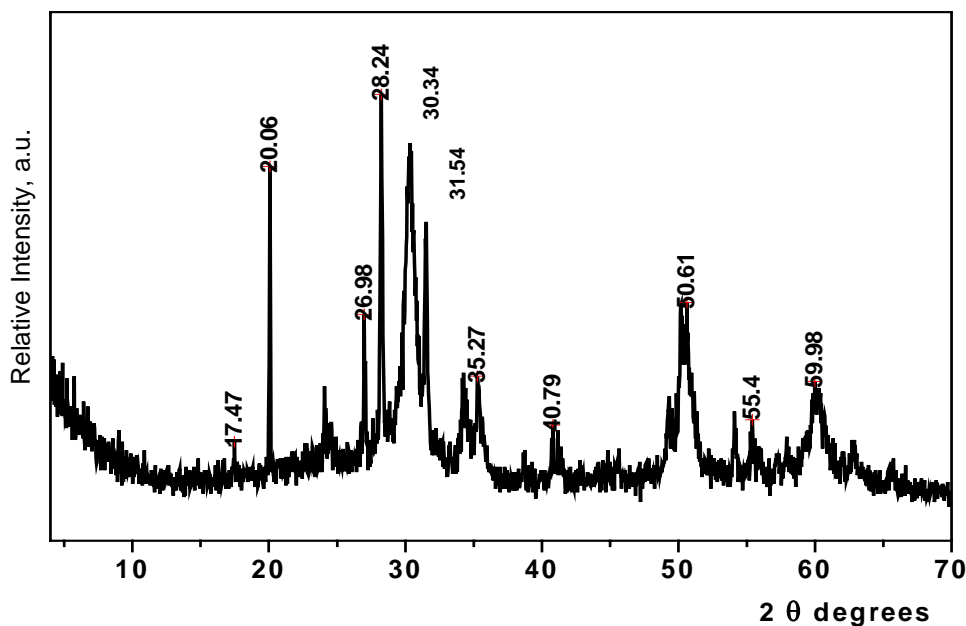


Figure 1. X-Ray Diffraction pattern of raw beach sand.

After the purification process, the zircon bulk was analyzed for crystallinity. The XRD spectrum showed only one mineral, zirconium silicate, presenting a high degree of crystallinity matching the JCPDS card 6-266 standard (Figure 3).

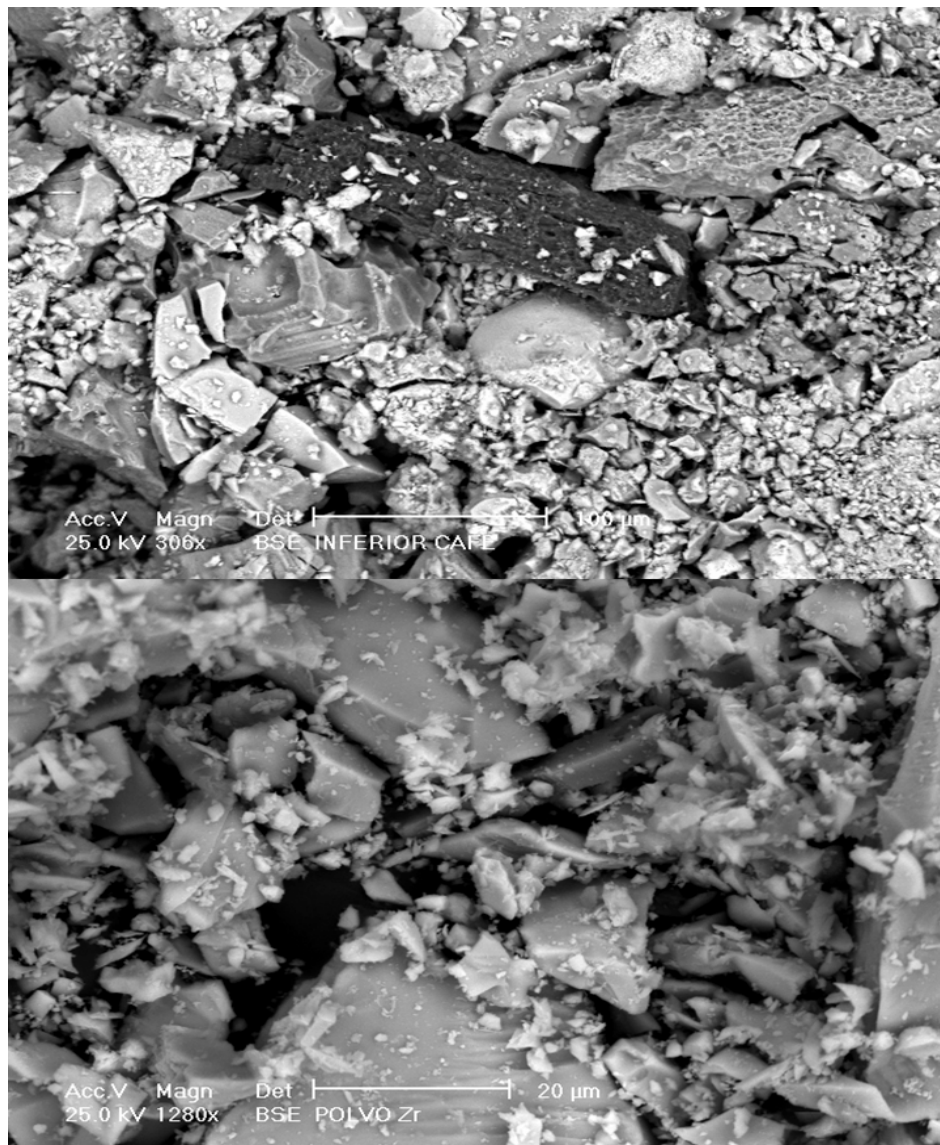


Figure 2. SEM micrography of raw beach sand.

### 3.2. Synthesis of zirconium hydrogen phosphate, $\alpha$ -ZP

The remaining acid liquor containing  $ZrF_4$  was slowly added to a 100 mL volume of 17 M phosphoric acid and distributed in four batches, each one under a different shaking condition, at controlled temperature, where the zirconium hydrogen phosphate was condensed.

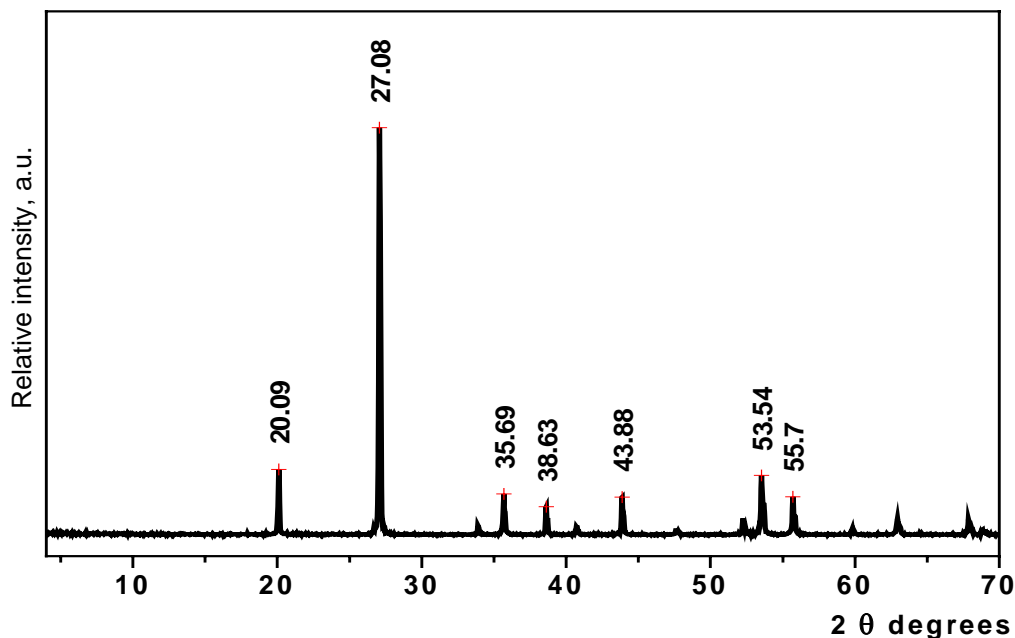


Figure 3. X-Ray Diffraction pattern of zirconium silicate

### 3.3. Characterization of the Materials

#### 3.3.1. $\alpha$ -ZP XRD Characterization

The intensity of diffracted X-rays from various planes as a function of  $2\theta$  value for the zirconium hydrogen phosphate  $\text{Zr}(\text{HPO}_4)_2 \cdot \text{H}_2\text{O}$  is showed. The main diffraction peaks are  $11.96^\circ$ ,  $25.01^\circ$ ,  $19.79^\circ$  and  $34.04^\circ$ . X-ray diffraction patterns showed that zirconium hydrogen phosphate is a powder with pure crystallographic phase, in agreement with JCPDS standard XRD card 34-0127 [12] (Figure 4). In the case of ZP250 and ZP500 the diffractograms shows a smaller peak displacement, probably due to a distance modification on lattice parameters (Figure 5).

#### 3.3.2. SEM analysis

SEM micrographs of the synthesized zirconium phosphate are shown. The resulting products were analyzed as for their morphology, showing a different particle shape in each batch. In the manual stirring batch, the  $\alpha$ -ZP particles (ZPMAN) were spherical with diameter ranging from 0.5 to 1  $\mu\text{m}$ . As shown in the image (Figure 6a), the surface of the spheres are smooth and this shape is homogeneous, which agree with that reported by Tarafdar *et al.* 2006 [10] and Kamiya *et al.*, 2006 [13]. Hexagonal platelets (ZP100) with an approximate average diameter of 1.5  $\mu\text{m}$  were observed at 100 rpm (Figure 6b).  $\alpha$ -ZP ordered aggregates (ZP250) of 20  $\mu\text{m}$

of size were identified at 250 rpm. These formed aggregates had a radial growing direction (Figure 6c). Finally, a condensed material (ZP500) with 20  $\mu\text{m}$  rolled platelets was observed at 500 rpm (Figure 6d). EDS measurements shown Zr, P and O in a 1:1:4 atom ratio, without contaminant elements. The particle shape and the growing of the  $\alpha$ -ZP crystal were the main differences observed. This may be due to the condensation reactions among hydroxyl groups of the water on adjacent spherical particles during agitation speed, to produce agglomerates of spherical particles. As the treatment agitation speed increased, the particle size increased too and the agglomerates obtained have largest dimensions.

### 3.3.3. TGA characterization

The thermogravimetric analysis of the condensed materials was performed at identical conditions in order to reveal the behavior of the materials as a function of the temperature and speed agitation (Figure 7). A total weight loss of 9.0% corresponding to a product with a  $\text{Zr}(\text{HPO}_4)_2 \cdot 0.5\text{H}_2\text{O}$  composition were observed in the TG curves of ZPMAN and ZP100 (Figure 5) in good agreement with the information reported by Alberti in 1994 [14].

The mass loss between 100 and 380°C, was attributed to 0.5 M crystallization water; the remaining water was lost between 380 and 680°C.

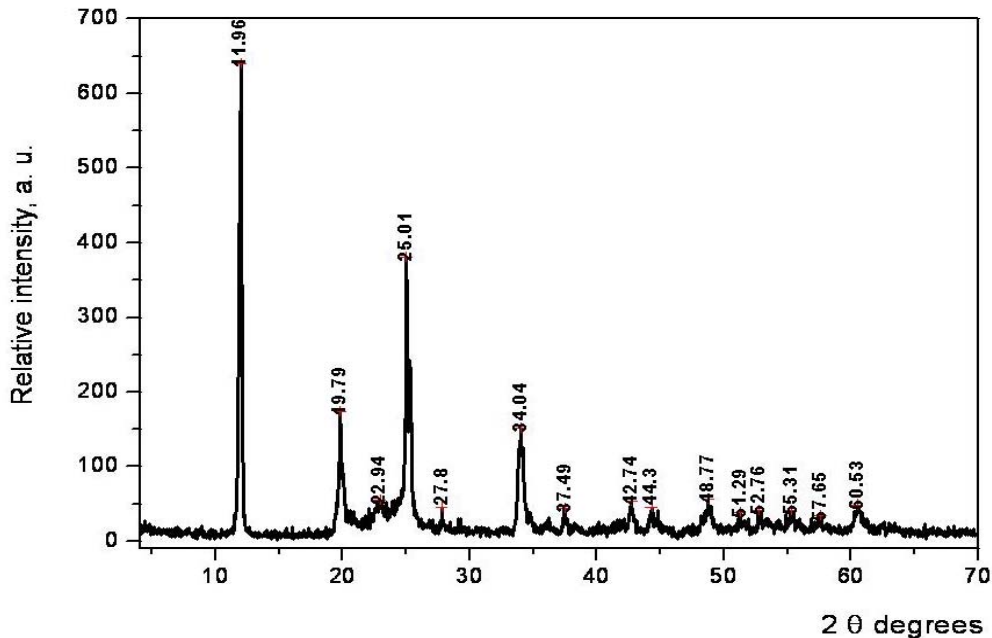


Figure 4. X-Ray Diffraction pattern of zirconium hydrogen phosphate,  $\alpha$ -ZP

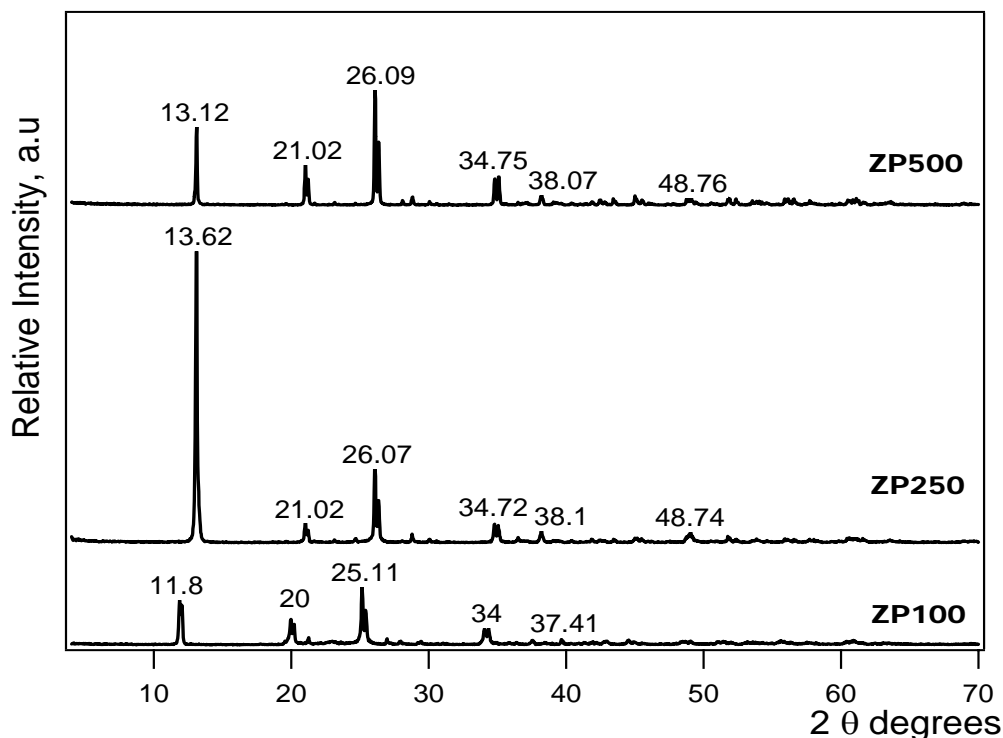
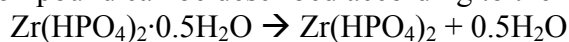


Figure 5. X-Ray Diffraction patterns of ZP100, ZP250 and ZP500

The dehydration of the compound can be described according to the following reactions:



The TG curve for ZP250 shows that sorbed water loss occurs between 110°C and 160°C, a weight loss that can be assigned to more than one water molecule. This fact indicated that the  $\text{Zr}(\text{HPO}_4)_2 \cdot 1.25\text{H}_2\text{O}$  compound was presented, adopting the anhydrous phase. Further heating produced the formation of zirconium pyrophosphate, as described by Constantino in 1997. The ZP500 TG curve shows that dehydration took place between 20 and 160°C, and that a second water loss occurred in two steps, namely, from 160 to 460°C and 460 to 680 °C. In both cases, the water loss corresponded approximately to one water molecule per formula unit, due to the dehydration and condensation of hydrogen phosphate into pyrophosphate [15].

Weight loss attributed to desorption of the surface adsorbed water which started below 100°C and subsequently curves showed broad endothermic peak with weight loss at around 150°C in all samples. Generally, the endothermic peak is ascribed to the formation of anhydrous phase. The second sharp endothermic peak without weight loss is then observed at 220°C associated with enantiotropic change of phase described by Slade et al., 1997 [16]. Further, heating lead to the formation of constituent water. All phases formed through the transformation from  $\alpha$ - $\text{Zr}(\text{HPO}_4)_2 \cdot \text{H}_2\text{O}$  to produced  $\text{ZrP}_2\text{O}_7$ .

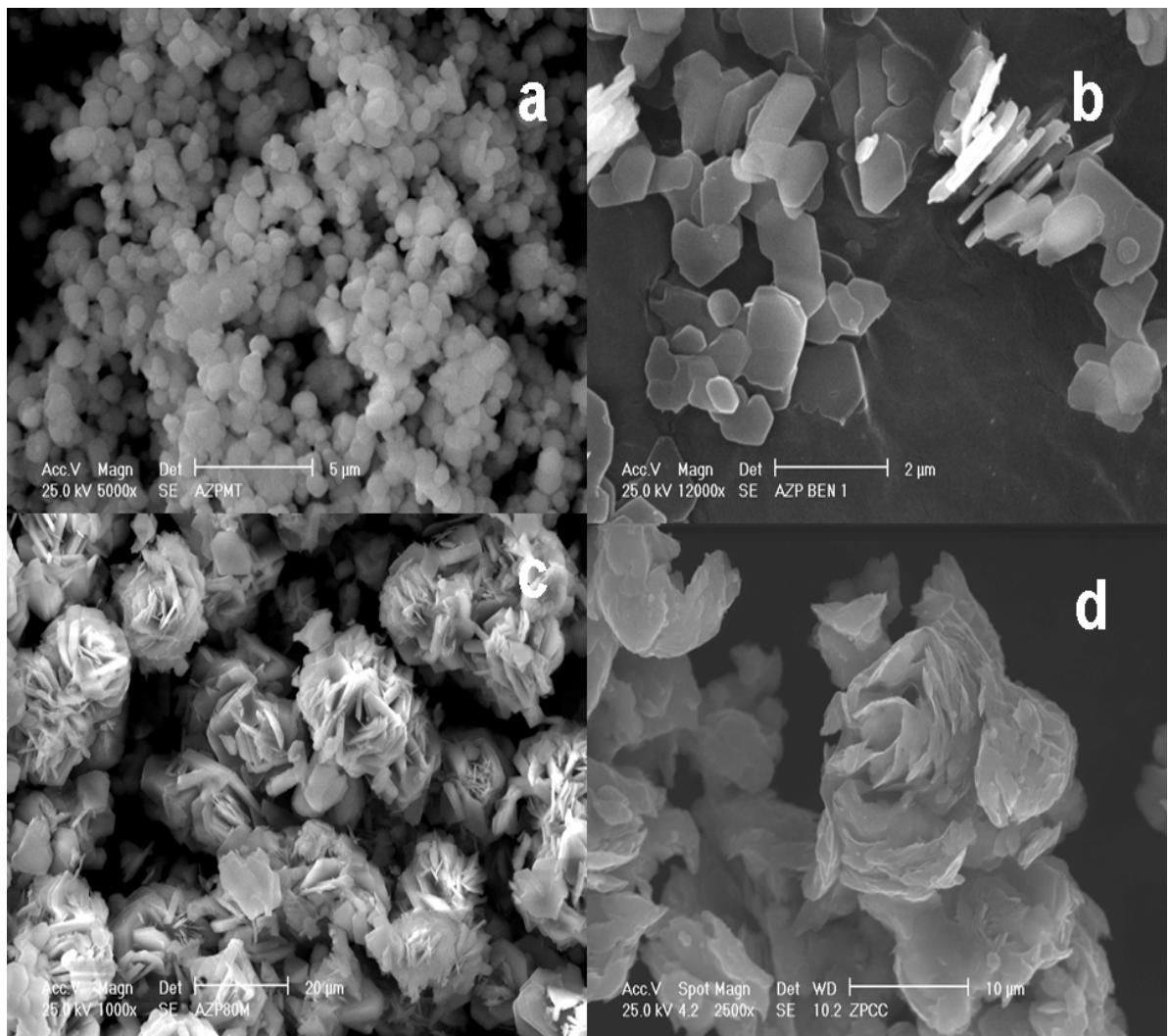


Figure 6. Images SEM of a.  $\alpha$ -ZP with manual agitation, b.  $\alpha$ -ZP condensed at 100 rpm, c.  $\alpha$ -ZP condensed at 250 rpm and d.  $\alpha$ -ZP condensed at 500 rpm.

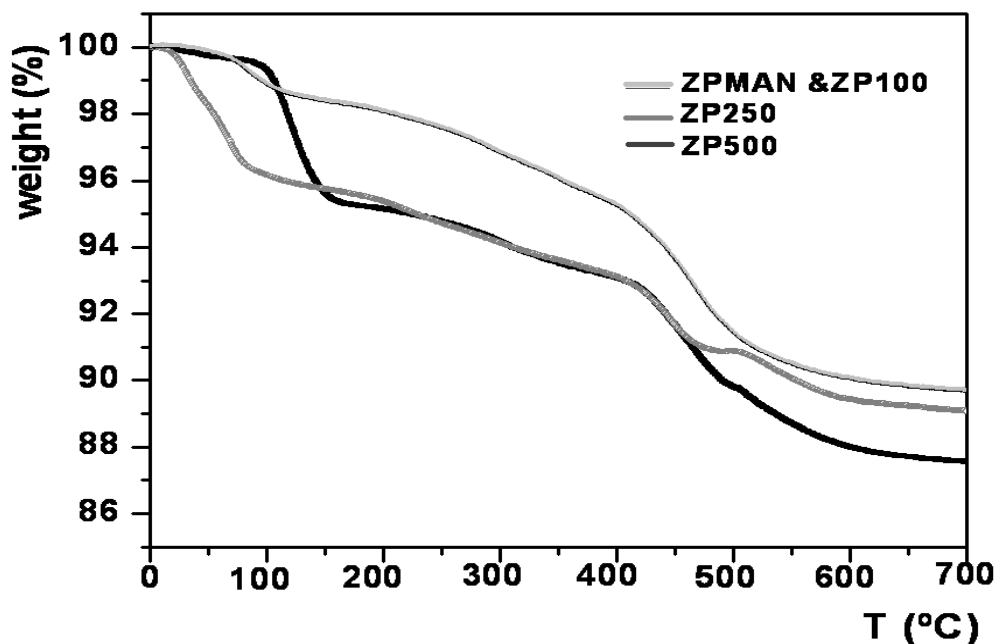


Figure 7. TGA curves of zirconium hydrogen phosphate,  $\alpha$ -ZP, at different agitation speeds.

### 3.3.4. BET determination

The BET specific area has been estimated through nitrogen adsorption-desorption measurement at liquid N<sub>2</sub> temperature in a relative pressure range of 0.05-0.95. The specific surface area of the  $\alpha$ -ZP is range from 4.30 until 5.77 m<sup>2</sup>g<sup>-1</sup> for the material obtained at several agitation speed, it is important to point out, though the agitation speed is different the values obtained for surface areas are not different. The results are summarized in Table 1.

Table 1. Specific surface areas determined from N<sub>2</sub>-BET

Zr(HPO <sub>4</sub> ) <sub>2</sub> ·H <sub>2</sub> O	Manual agitation	100 rpm	250 rpm	500 rpm
m <sup>2</sup> g <sup>-1</sup>	4.30	5.77	4.90	5.20

### 3.3.5. Infrared characterization

The corresponding FTIR spectra of the zirconium hydrogen phosphate,  $\alpha$ -ZP, obtained at different speed agitation were also obtained, as shown in Figure 8. The spectra exhibit the characteristics vibration bands from the phosphate group. The broad band between 3435 and 3418  $\text{cm}^{-1}$  has been attributed to asymmetric OH stretching of water molecule and the weak peak at around 1627  $\text{cm}^{-1}$  indicates the bending of water molecule, which is not proportionate with the total intensity of the corresponding stretching band. A strong sharp band centered at 1062  $\text{cm}^{-1}$  corresponds to P-O stretching vibration for ZPMAN and ZP100. The bands at 596 and 525  $\text{cm}^{-1}$  attributed to deformations modes of  $\text{PO}_4^{3-}$  [10, 17, 18]. The distorted band at 1060-1100  $\text{cm}^{-1}$  in corresponds to some distorted tetrahedral phosphate groups in the nuclei of zirconium phosphates for the influence of the speed agitation during the forming of the products. In the case of ZP250 and ZP500, it was observed one absorption band at 737 and 745  $\text{cm}^{-1}$  respectively corresponding to P-O-P vibration of the diphosphate groups ( $\text{O}_3\text{P-O-PO}_3$ ). Finally, the observed bands to 1124 and 1113  $\text{cm}^{-1}$  and 546 and 544  $\text{cm}^{-1}$  from ZP500 and ZP250 correspond to the deformation vibrations of P-O bonding of the  $\text{PO}_3$  terminal groups. In agreement with the obtained results, the picks deformations as well as the displacement in the positions of some of them, must to the mechanical differences of the materials obtaining which plays an important role in the samples crystallization.

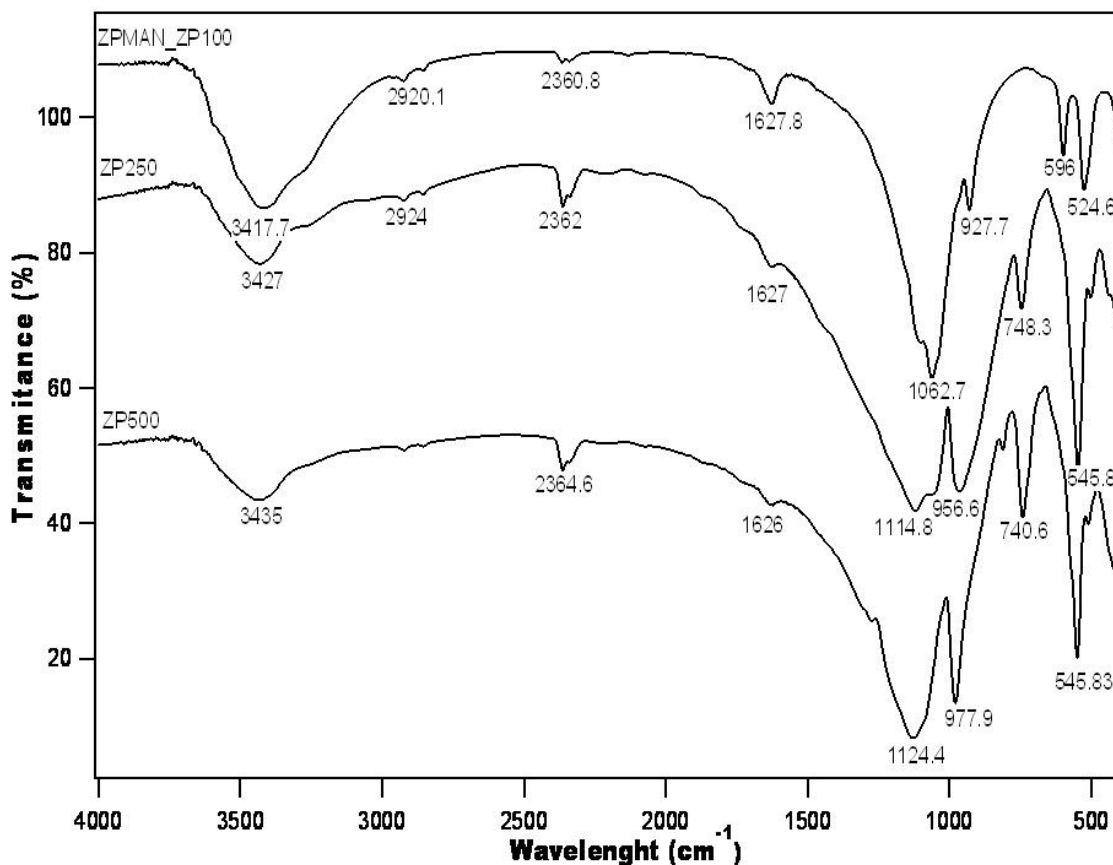


Figure 8. IR spectra of zirconium hydrogen phosphate at different agitation speeds.

#### 4. CONCLUSIONS

Zircon and zirconium hydrogen phosphate were successfully obtained from Mexican Pacific beach sand. The technique followed in the sand purification was adapted with a view to obtaining several products out of a raw material that is abundant in México. It is interesting to point out that this technique provides an easy way to obtain highly pure zircon with great homogeneity in its grain size. The zirconium hydrogen phosphate presented forms of crystallization according to the agitation speed that prevailed during its condensation process, because crystallization water changes according to this parameter, leading to the presence of  $\alpha$ -ZP in different hydrated phases. Spherical particles of  $\alpha$ -ZP was prepared through an easy, convenient and economical route. This method has more advantages not only for inexpensive starting materials and shorter production times but also for the better control over the morphology of the synthesized materials.

#### ACKNOWLEDGEMENTS

This project is supported by the CONACYT, under contract 36348-E.

#### REFERENCES

- [1] Ordoñez, R. E., Drot, R. and Simoni, E., 2002, "Sorption of uranium (VI) onto lanthanum phosphates surfaces." *Langmuir*, Vol. 18, pp. 7977-7984.
- [2] Constantino U., 1997, "Thermoanalytical Study, Phase transitions and dimensional changes of  $\alpha$ -Zr (HPO<sub>4</sub>)\*H<sub>2</sub>O Large Crystals." *J. Solid State Chem.*, Vol., **132**, pp. 17-23.
- [3] Krogh A. and Andersen M., 1998, "Preparation and characterization of a new 3-dimensional Zirconium Hydrogen Phosphate,  $\tau$ -Zr(HPO<sub>4</sub>)<sub>2</sub> Determination of the complete Crystal structure Comparing synchrotron X-ray single crystal Diffraction and Neutron Powder Diffraction". *Inorg. Chem.*, Vol., **37**, pp. 876-881.
- [4] Souka N., Shabana R., Farah K., 1976, "Adsorption behaviour of some actinides on zirconium phosphate stability constant determinations." *J. Radional. Nucl. Ch.*, Vol., **33**, pp. 215-222.
- [5] Chunli L., 2001, "The migration of radionuclides <sup>237</sup>Np, <sup>238</sup>Pu and <sup>241</sup>Am in a weak loss aquifer: A field column experiment." *Radiochim. Acta*, Vol., **89**, pp. 519-522.
- [6] Drot R., Lindecker C., Fourest B., Simoni E., 1998, "Surface characterization of zirconium and thorium phosphate compounds." *New J. Chem.* pp. 1105-1109.
- [7] Lomenech C., Drot R. and Simoni E., 2003, "Speciation of uranium (VI) at the solid/solution interface: sorption modeling on zirconium oxide." *Radiochim Acta*, Vol., **91**, pp. 453-461.
- [8] Hirai, H., Toshiyuki, N., Imanaka, N., Adachi G. Y. , 2004, "Characterization and thermal behavior of amorphous rare earth phosphates." *J. Alloys Compound*, Vol., **374**, pp. 84-88.
- [9] Vaivars G., Maxakato N. W., Mokrani T., Petrik L., Klavins J., Gericke G., Linkov V., 2004, "Zirconium phosphate based inorganic direct methanol fuel cell." *Materials Science*, Vol., **10(2)**, pp. 162-165.

- [10] Tarafdar A., Panda A. B., Pradhan N. C. and P. Pramanik, 2006, Synthesis of spherical mesostructured zirconium phosphate with acidic properties. *Microporous and mesoporous materials*, Vol. 95(1-3), pp. 360-365.
- [11] Clearfield A, Stynes J. A., 1964, "The preparation of crystalline zirconium phosphate and some observations on its ion exchange behavior." *J. Inorg. Nucl. Chem.*, Vol., **26**, pp. 117-129.
- [12] Bayliss, P., 1986, Mineral Powder Diffraction File Date Book, JCPDS (Swarthmore, PA).
- [13] Kamiya, M., Sasai, R. and Itoh, H., 2006, "Lead recovery from  $\text{PbZrO}_3$  using wet ball-mill technique and hydrothermal synthesis of  $\alpha$ -zirconium phosphate from wastewater for resource recovery." *Journal of Hazardous Materials*, Vol. B134, pp. 67-73.
- [14] Alberti G, Constantino U, Millini R, Perego G, Vivian R., 1994, "Preparation, characterization, and structure of  $\alpha$ -zirconium hydrogen phosphate hemihydrate." *J. Solid State Chem.*, Vol. 113, pp. 289-295.
- [15] Pecharrómán C., Ocaña M., Tartaj P., Serna C. J., 1994, "Infrared optical properties of zircon." *Mater. Res. Bull.* Vol. 29, pp. 417-426.
- [16] Slade, R. C. T., Knowles, J. A., Jones, D. J., Roziere, J, 1997, "The isomorphous acid salts  $\alpha$ - $\text{Zr}(\text{HPO}_4)_2 \cdot \text{H}_2\text{O}$ ,  $\alpha$ - $\text{Ti}(\text{HPO}_4)_2 \cdot \text{H}_2\text{O}$  and  $\alpha$ - $\text{Zr}(\text{HAsO}_4)_2 \cdot \text{H}_2\text{O}$ ." *Solid State Ionics*, Vol. 96, pp. 9-19.
- [17] Williams, D. H. and Fleming, I., **1980**, "Spectroscopic methods in organic chemistry." McGraw-Hill Book Company. UK. 251 p.
- [18] Alamo J., Roy R., 1984, "Revision of Crystalline Phases in the system  $\text{ZrO}_2$ - $\text{P}_2\text{O}_5$ ." *Communications of the American Ceramic Society*, Vol. 67, pp. 80-82.